Cold Denaturation and Heat Denaturation of *Streptomyces* Subtilisin Inhibitor. 1. CD and DSC Studies†

Atsuo Tamura, Kazuo Kimura, Hideki Takahara, and Kazuyuki Akasaka*
Department of Chemistry, Faculty of Science, Kyoto University, Kyoto 606, Japan
Received May 29, 1991; Revised Manuscript Received August 14, 1991

ABSTRACT: Cold denaturation and heat denaturation of the protein *Streptomyces* subtilisin inhibitor (SSI) were studied in the pH range 1.84–3.21 and in the temperature range −3–70 °C by circular dichroism and scanning microcalorimetry. The native structure of the protein was apparently most stabilized at about 20 °C and was denatured upon heating and cooling from this temperature. Each denaturation was reversible and cooperative, proceeding in two-state transitions, that is, from the native state to the cold-denatured state or from the native state to the heat-denatured state. The two denatured states, however, were not perfect random-coiled structures, and they differed from each other, indicating that there exist three states in this temperature range, i.e., cold denatured, native, and heat denatured. The difference between the cold and heat denaturations was indicated first by circular dichroism. The isodichroic point for the transition from the native state to the cold-denatured state was different from that from the native state to the heat-denatured state in the pH range between 3.21 and 2.45. Moreover, molar ellipticity for the cold-denatured state was different from that of the heat-denatured state, and the transition from the former to the latter was observed at pH values below 2. Values of van't Hoff enthalpies from the native state to the heat-denatured state at pH values between 3.21 and 2.45 were obtained by curve fitting of the CD data, and ΔC_p = 1.82 (±0.11) [kcal/(mol·K)] was obtained from the linear plot of the enthalpies against temperature. The parameters obtained from the heat denaturation studies gave curves for $\Delta G°$ which were not in agreement with the experimental data in the cold denaturation region when extrapolated to the low temperature. Moreover, the value of the apparent ΔC_p for the cold denaturation in the pH range 3.03–2.45 was estimated to be different from that for the heat denaturation, indicating that the mechanism of the cold denaturation of SSI is different from a simple cold denaturation. A differential scanning calorimetric study confirmed that the heat denaturation was of the cooperative two-state type (from the dimeric form in the native state to the monomeric form in the heat-denatured state) with absorption of enthalpy upon increasing the temperature at pH 3.07. As the pH decreased, however, the enthalpy for the heat denaturation decreased whereas that for the cold denaturation showed a different behavior. The value of the heat capacity of the protein in the cold-denatured state is different from that in the heat-denatured state and is even closer to that in the native state. Furthermore, below pH 2, a direct transition between the two denatured states was observed with absorption of heat.

It has been known for some time that the native structure of a globular protein in an aqueous environment may be destroyed not only with increasing temperature (heat denaturation) but also with decreasing temperature (cold denaturation; Brandts & Hunt, 1967; Pace & Tanford, 1968; Privalov & Gill 1988; Privalov, 1989). The phenomenon of cold denaturation has been firmly established recently in two proteins, i.e., in myoglobin (Privalov et al., 1986) and staphylococcal nuclease (Griko et al., 1988). These are relatively small single-domain proteins with no disulfide bridges.

Streptomyces subtilisin inhibitor [SSI;[1] MW = 23000, p*I* (isoelectric point) = 4.3, α content = 13%, β content = 24%; Hiromi et al., 1985) is a dimeric protein consisting of two identical subunits, each having two disulfide bridges. In the present report, SSI was also found to undergo cold denaturation in an acidic aqueous environment and the thermodynamic parameters of the heat and the cold denaturation of SSI were examined in detail using circular dichroism and microcalorimetry. Since, so far, cold denaturation has not been studied in a protein having subunits and disulfide bridges, SSI is thought to provide an interesting system of study and may disclose some new aspects. The results will be compared with those obtained with myoglobin and staphylococcal nuclease.

Both the heat and cold denaturations were examined first by circular dichroism (CD) in glycine buffers (pH 1.84–3.21), and van't Hoff enthalpy (ΔH_{vH}) and heat capacity changes (ΔC_p) were obtained. The thermodynamic parameters thus obtained were used for further analysis of the denaturation on the assumption of the denaturational equilibrium $N_2 \rightleftharpoons 2D$, where N_2 represents the dimeric form of the native structure of SSI and D represents the denatured state of the monomeric form of SSI (Takahashi & Sturtevant, 1981). Calorimetric measurements were also performed to confirm the thermodynamic analysis of the CD data.

Materials and Methods

Crude solutions of SSI were obtained by cultivating *Streptomyces albogriseolus* S-3253 and were purified on chromatographic columns with DE52 (Whatman) and Sephacryl S-200 (Pharmacia), as originally described by Sato and Murao (1973). Protein solutions for CD measurements were prepared by dissolving appropriate amounts of lyophilized SSI in 25 mM glycine buffer at the desired pH. The solution

†This work was supported by a Grant-in-Aid for Developmental Scientific Research from the Ministry of Education, Science, and Culture of Japan.

[1] Abbreviations: SSI, *Streptomyces* subtilisin inhibitor; CD, circular dichroism; DSC, differential scanning calorimetry.

0006-2960/91/0430-11307$02.50/0

was centrifuged for 10 min at 15000 rpm and filtered through a polysulfone membrane filter (pore size 0.2 μm; Gelman Science). For DSC measurements, the protein solutions were further dialyzed against the glycine buffers. The protein concentrations were determined spectrophotometrically after diluting the solution in a concentrated phosphate buffer (0.10 M, pH 7.2), using the absorbance $A_{0.1\%} = 0.796$ at 280 nm (Inouye et al., 1977).

CD spectra in the range of 180–350 nm were measured with a Jasco J-720 spectropolarimeter using a cell with a light path of 0.5 mm. The protein concentration was kept at 0.368 mg/mL (1.60×10^{-5} M) throughout. The temperature of the solution was changed with a step of about 4 °C with time intervals of 20 min.

The calorimetric measurements were made with a scanning calorimeter DASM-4 (Privalov & Potekhin, 1986) in a temperature range from 0 to 80 °C. The temperature scanning rate was set at 1 K/min. The protein concentration varied from 3.59 to 4.26 mg/mL in the same glycine buffers as those used in the CD measurements.

Results and Discussion

CD Measurements. Temperature dependences of the CD spectra were measured in the temperature range between −2.9 and 70 °C with about 4 °C steps at intervals of 20 min, in 25 mM glycine buffers, pH 3.21, 3.03, 2.87, 2.72, 2.45, 2.21, 2.08, and 1.84. Reversibility of the denaturations was confirmed by comparing the CD spectra measured in the first run with those obtained with repeated scans, in going from −2.9 to 19.8 °C or from 70.0 to 19.8 °C at each pH. The molar ellipticities obtained in the second run reproduced those in the first run within experimental error, showing that the reversibility was essentially complete. The temperature-scanning rate was chosen to be sufficiently slow so that the conformational states involved are in equilibrium at each temperature. The CD spectrum was fully reproduced when the protein solution was brought up to 19.8 °C from −2.9 °C at a much higher rate (22.7 deg/20 min) after leaving the protein solution at −2.9 °C for a sufficiently long time (45 min). This result indicates that the rate of folding from the cold-denatured state to the native state is sufficiently rapid even at the temperature-scanning rate of 1.1 K/min.

Panels a–e of Figure 1 show the CD spectral changes with temperature at pH 2.87 (a, the high-temperature side; b, the low-temperature side), at pH 2.45 (c, the high-temperature side; d, the low-temperature side), and at pH 1.84 (e, the whole temperature region). The CD spectral changes of Figure 1a occur with a clear isodichroic point at 208.3 nm, whereas those of Figure 1b occur with a clear isodichroic point at a slightly but distinctively different wavelength, 209.6 nm. The existence of these isodichroic points suggests that these two transitions proceed as two-state processes; the former can be identified as the conformational transition of SSI between the native state and the heat-denatured state (heat denaturation), and the latter can be identified as that between the native state and the cold-denatured state (cold denaturation). The CD spectral changes in Figure 1c, with almost the same isodichroic points (207.8 nm for the low-temperature transition and 209.9 nm for the high-temperature transition), can be identified also with the heat and cold denaturations, respectively. The shapes of the CD spectra at around 20 °C are different between pH 2.87 and 2.45 because of the difference in the native fraction at the two pH values. At pH 1.84 (Figure 1e), CD spectral changes are different from those at pH 2.87 and 2.45. Only relatively small spectral changes were observed with two isodichroic points (205.0 and 231.7 nm), entirely different from those at the other two pH values. This transition is interpretable as that from the cold- to the heat-denatured state, as will be discussed later.

The CD spectra at various pH values converge to a common pattern at high temperatures, indicating that the heat-denatured conformation is common to every pH. Similarly, the spectra tend to converge to a common spectrum at low temperatures below pH 2.21, indicating that in the cold-denatured state the protein takes a definite structure irrespective of the pH of the measurements. Figure 1f represents typical CD patterns for the fully native (N; pH 3.21, 19.8 °C), fully heat-denatured (D; pH 2.21, 50.3 °C), and the fully cold-denatured states (D′; pH 2.21, −2.9 °C). The spectrum for the native state and that for the heat-denatured state cross at 208.2 nm, and the spectrum for the native state and that for the cold-denatured state cross at 209.8 nm, at nearly identical wavelengths for the respective isodichroic points for the heat denaturation and the cold denaturation at pH 2.87 and 2.45. The crossing points between the cold- and heat-denatured states come at 204.7 and 231.5 nm, which correspond approximately to the isodichroic points observed at pH 2.08 (205.4 and 231.0 nm) and at pH 1.84 (205.0 and 231.7 nm; Figure 1e), supporting the view that the observed transition at pH 1.84 is that from the cold- to the heat-denatured state.

Figure 2 shows the plot of isodichroic points vs pH. The isodichroic points for the cold denaturation and the heat denaturation are slightly but distinctly different from each other and are constant at averaged values of 209.8 and 208.1 nm, respectively. This observation suggests strongly that the heat-denatured and the cold-denatured states are different in secondary structure. At pH 2.21, isodichroic points were not clear, especially below 25 °C (cf. Figure 3d), suggesting that the equilibrium involves more than two states, i.e., the cold-denatured, the heat-denatured, and the native states. The isodichroic point for cold denaturation at pH 3.21 is excluded because the spectral changes were too small to obtain a reliable value (cf. Figure 3a).

Thermodynamic Analysis of the CD Data. The molar ellipticities from 222 nm (at which the α helix takes a minimum value of θ; Johnson, 1990) to 197 nm (at which the β sheet and the random coil take maximum and minimum values of θ, respectively) were plotted as functions of temperature, at every 5-nm interval excluding 207 nm, where a clear transition was hard to recognize due to the closeness to the isodichroic point. Figure 3 shows the plots for pH 3.21, 2.87, 2.45, and 1.84 as examples. The maximum near 20 °C indicates the dominance of the native structure, while the decline of the ellipticity either toward the higher temperature side or toward the lower temperature side shows the transition from the native structure to the heat-denatured structure or from the native structure to the cold-denatured structure. The cold and heat denaturations occur at almost the same temperatures irrespective of the wavelength of observation (222–197 nm), indicating clear cooperativity of unfolding of the entire secondary structure of SSI.

According to the denaturational equilibrium

$$N_2 \rightleftharpoons 2D \quad K = [D]^2/[N_2] \qquad \text{(for heat denaturation)} \tag{1}$$

$$N_2 \rightleftharpoons 2D' \quad K' = [D']^2/[N_2] \qquad \text{(for cold denaturation)} \tag{2}$$

where N_2 represents the native conformation of SSI (as a dimer) and D and D′ represent the heat- and cold-denatured conformations (as monomers), respectively, curve fitting of the ellipticity was carried out by the following procedure: The

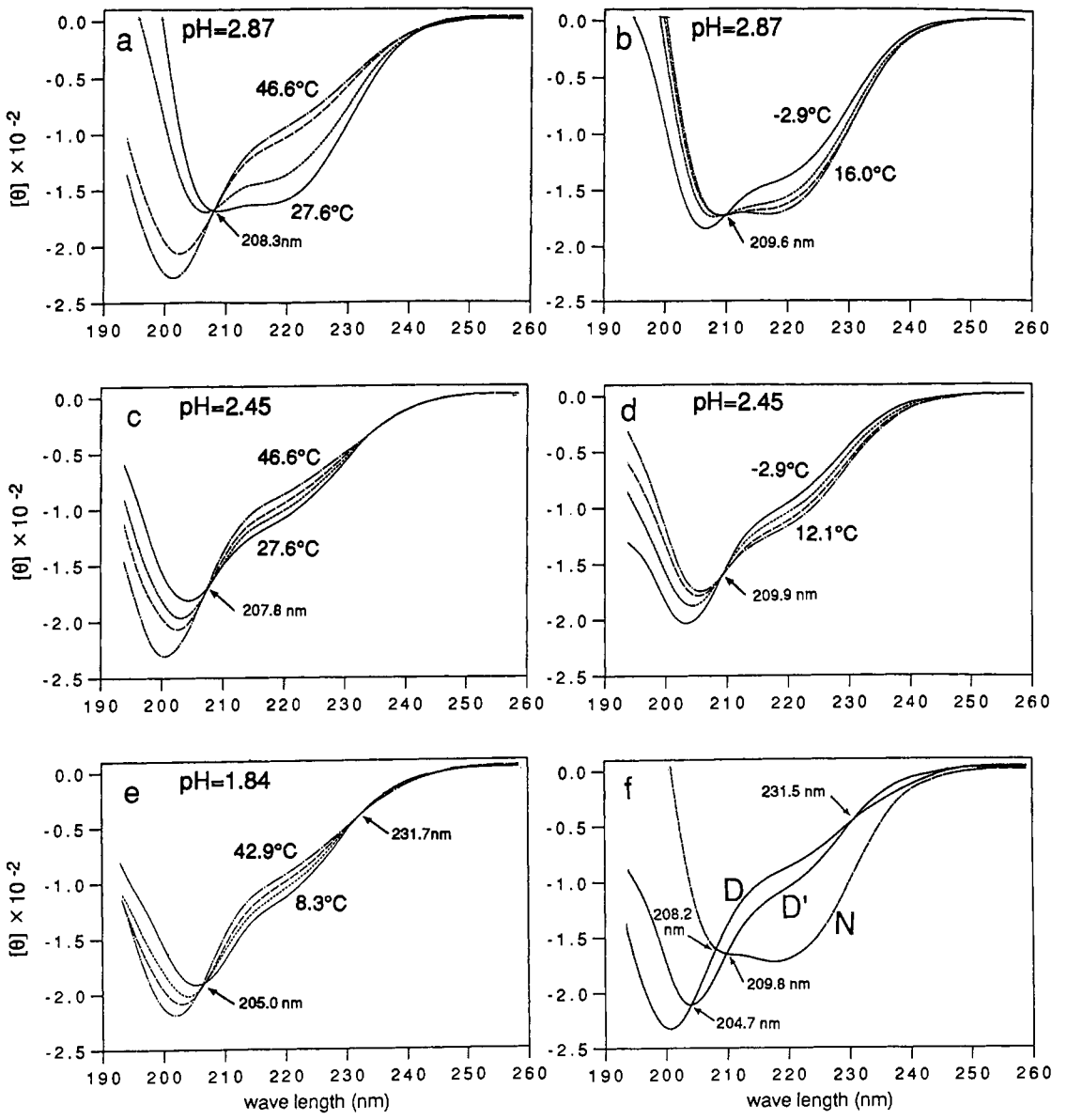

FIGURE 1: Circular dichroism spectra of SSI near the transition temperatures at various pH values in 25 mM glycine buffers. (a) pH 2.87 (high-temperature region: 27.6, 35.3, 42.9, 46.6 °C); (b) pH 2.87 (low-temperature region: 16.0, 8.3, 4.6, −2.9 °C); (c) pH 2.45 (high-temperature region: 27.6, 31.5, 35.3, 46.6 °C); (d) pH 2.45 (low-temperature region: 12.1, 8.3, 4.6, −2.9 °C); (e) pH 1.84 (8.3, 27.6, 39.2, 46.6 °C). The arrows indicate isodichroic points. (f) CD spectra of SSI in fully cold-denatured (D'), fully heat-denatured (D), and fully native (N) states.

experimentally observed ellipticity (θ) is assumed to be expressed by the superposition of the cold and heat denaturations as

$$\theta = \theta_{N2} + \alpha(2\theta_D - \theta_{N2}) + \beta(2\theta_{D'} - \theta_{N2}) \quad (3)$$

where θ_{N2}, $2\theta_D$, and $2\theta_{D'}$ are the molar ellipticity of SSI in the native, the heat-denatured state, and the cold-denatured state, respectively, and α and β are degrees of dissociation expressed by using equilibrium constants as

$$\alpha = (K/8c) \times [((1 + (K'/K)^{1/2})^2 + 16c/K)^{1/2} - (1 + (K'/K)^{1/2})] \quad (4)$$

$$\beta = (K'/8c)[((1 + (K/K')^{1/2})^2 + 16c/K')^{1/2} - (1 + (K/K')^{1/2})] = \alpha(K'/K)^{1/2} \quad (5)$$

where c is the initial concentration of SSI solution (1.60×10^{-5} mol/L). The temperature dependence of the ellipticity should be expressed by the van't Hoff equations as

$$K = A \exp(-\Delta H_{vH}/RT) \quad (6)$$

$$K' = A' \exp(-\Delta H'_{vH}/RT) \quad (7)$$

where ΔH_{vH} and $\Delta H'_{vH}$ are the van't Hoff enthalpies for the heat and cold denaturations, A and A' are constants, R is the gas constant, and T is the absolute temperature.

Temperature dependences of the experimentally observed ellipticities at each wavelength were fitted by using eqs 3–7. The parameters for the curve fitting were as follows: The values of molar ellipticity adopted for θ_{N2}, $2\theta_D$, and $2\theta_{D'}$ are those at pH 3.21 and 20 °C, where most of the SSI molecules are supposed to be in the native conformation (Figure 3a), those at pH 2.21 and 61.5 °C, where the ellipticity is assumed to reach the converged value at a higher temperature (heat denatured), and those at pH 2.21 and −2.9 °C, where the ellipticity is assumed to reach another converged value at lower temperature (cold denatured), respectively. The values actually employed are θ_{N2} = −1.81, −1.91, −1.82, −0.28, and 1.90 ($\times 10^{-2}$ (deg·cm^2)/mol, for 222, 217, 212, 202, and 197 nm, respectively), $2\theta_D$ = −0.82, −0.97, −1.20, −2.33, and −2.07, and $2\theta_{D'}$ = −0.96, −1.14, −1.37, −1.82, and −1.32. The values for $2\theta_D$ and $2\theta_{D'}$ are close to but different from each other, as the transition from the former to the latter is observed at pH 1.84 (Figure 2e). Thus, in view of the secondary structure as

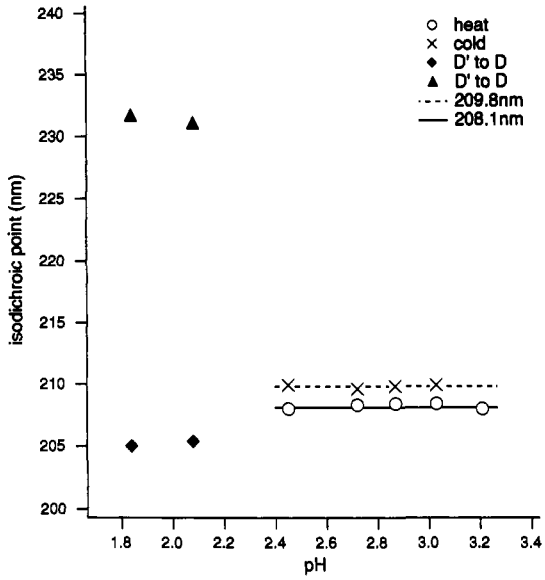

FIGURE 2: Plot of the isodichroic points against the pH between N and D (○), N and D′ (×), and D′ and D (▲ and ◆).

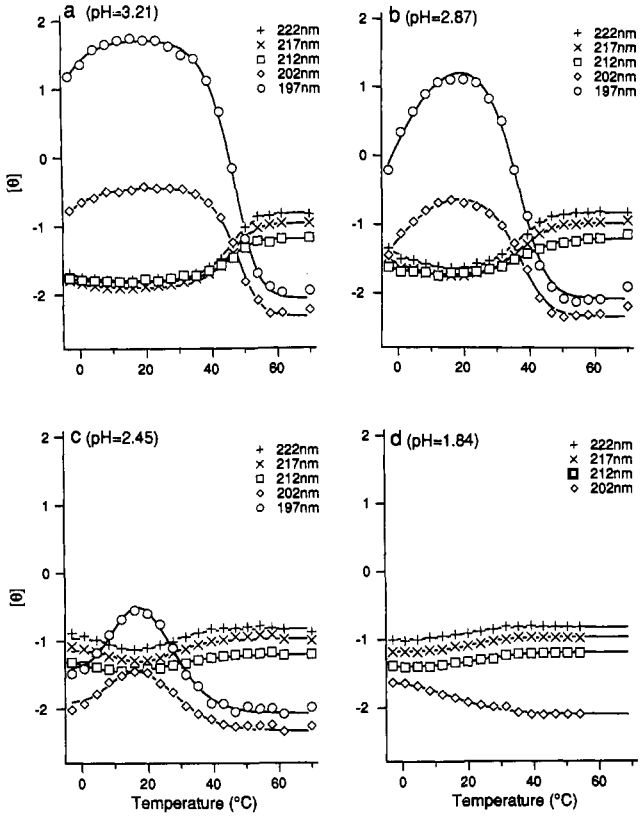

FIGURE 3: Temperature dependences of the molar ellipticity at 222 nm (+), 217 nm (×), 212 nm (□), 202 nm (◇), and 197 nm (○). The full-drawn curves were obtained by least-squares fitting of eq 3 to the experimental data. (a) pH 3.21. (b) pH 2.87. (c) pH 2.45. (d) pH 1.84. (Fitting to the 197-nm data were abondoned at pH 1.84, because of a poor signal-to-noise ratio.)

revealed by CD, the structure of SSI in the cold-denatured state is close to but a little different from that in the heat-denatured state. The curve fitting was carried out by the method of least squares, and the result is displayed in Figure 3 as full-drawn curves. The simulations are fairly well fitted to the experimental values in the pH range 3.21–2.45, while it is difficult in practice to fit the data of pH 2.08 and 1.84. Thus, the data at pH 1.84 are fitted by a single transition (from D′ to D) as in Figure 3d. The coincidence between the experimental data and the fitted curves indicates the validity of the conditions for the simulation including the assumption of eq 1 and 2. That SSI dissociates into subunits both upon heat and cold denaturations will be shown directly by sedimentation equilibrium experiments in the following paper (Tamura et al., 1991).

Table I: Summary of Heat and Cold Denaturation Temperatures (T_d and T'_d) and Associated van't Hoff Enthalpies (ΔH_{vH} and $\Delta H'_{vH}$) Obtained by Curve Fitting of the CD Data at Various Wavelengths

wavelength (nm)	222	217	212	202	197	av
			pH 3.21			
T_d (°C)	45.4	45.3	44.7	47.4	46.4	45.8
ΔH_{vH} (kcal/mol)	72.0	70.9	74.8	80.3	75.5	74.7
T'_d (°C)	−11.5	−11.3	−11.9	−9.1	−9.9	−10.7
$\Delta H'_{vH}$ (kcal/mol)	−49.2	−49.2	−48.3	−44.8	−50.5	−48.4
			pH 3.03			
T_d (°C)	38.4	37.7	34.8	42.7	41.1	38.9
ΔH_{vH} (kcal/mol)	56.8	58.3	56.7	67.2	59.3	59.7
T'_d (°C)	−0.9	−0.7	2.4	−8.8	−9.9	−3.6
$\Delta H'_{vH}$ (kcal/mol)	−38.0	−25.0	−39.1	−41.1	−25.8	−33.8
			pH 2.87			
T_d (°C)	35.0	35.5	36.4	35.9	35.5	35.7
ΔH_{vH} (kcal/mol)	49.8	49.5	45.8	57.7	57.8	52.1
T'_d (°C)	−2.4	−2.1	−5.8	0.8	0.3	−1.8
$\Delta H'_{vH}$ (kcal/mol)	−24.8	−24.7	−20.5	−36.5	−29.6	−27.2
			pH 2.72			
T_d (°C)	31.3	31.6	33.8	30.8	30.5	31.6
ΔH_{vH} (kcal/mol)	46.0	46.0	44.4	47.7	50.3	46.9
T'_d (°C)	3.5	3.8	3.4	5.5	4.3	4.1
$\Delta H'_{vH}$ (kcal/mol)	−34.8	−34.8	−29.8	−38.4	−35.1	−34.6
			pH 2.45			
T_d (°C)	20.0	21.5	21.6	23.0	22.0	21.6
ΔH_{vH} (kcal/mol)	31.9	31.7	23.7	31.0	31.8	30.0
T'_d (°C)	13.9	14.7	13.8	12.7	13.8	13.8
$\Delta H'_{vH}$ (kcal/mol)	−46.4	−46.1	−39.5	−48.7	−46.7	−45.5

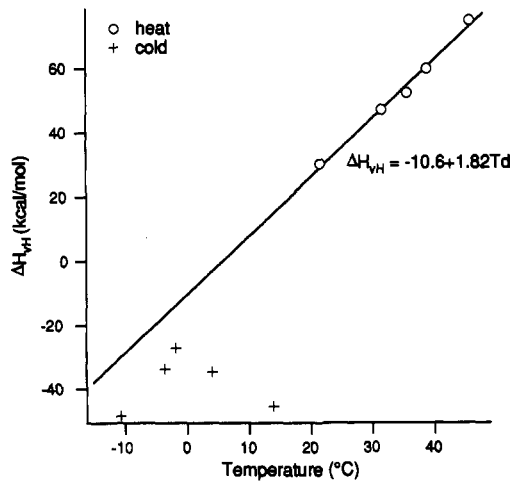

FIGURE 4: Plot of the van't Hoff enthalpies (ΔH_{vH}) obtained from the analysis of the CD data against denaturation temperatures, for heat denaturation (○) and cold denaturation (+).

Table I summarizes the enthalpies (ΔH_{vH}, heat denaturation; $\Delta H'_{vH}$, cold denaturation) and denaturation temperature (T_d, heat denaturation; T'_d, cold denaturation) at various pH values obtained by this simulation. T_d and T'_d are defined here as temperatures where $\alpha = 0.5$ and $\beta = 0.5$, respectively. [In contrast to a monomeric protein (Privalov, 1979), $\Delta G°$ is not zero at T_d or T'_d for a dimeric protein such as SSI.] T_d and T'_d are independently calculated from the results of the simulation using the values A and ΔH_{vH} for T_d, and A' and $\Delta H'_{vH}$ for T'_d.

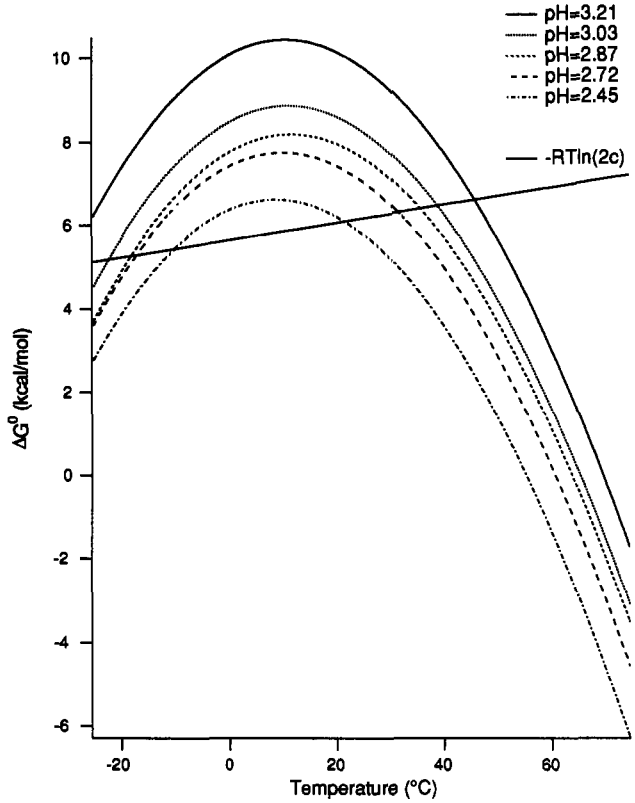

FIGURE 5: Differences in standard Gibbs energy ($\Delta G°$) between the native and denatured states of SSI as functions of temperature at various pH values, calculated from eq 8 with the values of ΔC_p and ΔH_{vH} obtained in Figure 4.

The averaged values of enthalpy are plotted against denaturation temperatures (T_d) in Figure 4 in a range from pH 3.21 to 2.45. (The value at pH 2.21 is only of the heat denaturation because the transition of the cold denaturation was not clear at this pH as described earlier.) Since the plot shows clear linearlity, ΔC_p for the heat denaturation, defined here as the slope of the plot of Figure 4, is obtained as 1.82 (±0.11) kcal/(mol·K). By using these values, the standard Gibbs energy difference ($\Delta G°$) of the native and denatured states of SSI at various pH values can be obtained according to the equation

$$\Delta G°(T) = \Delta H°(T_d) - T(\Delta H°(T_d) - \Delta G°(T_d))/T_d + \Delta C_p(T - T_d - T \ln(T/T_d)) \quad (8)$$

which is derived from the assumption of constancy of ΔC_p over the experimental range of temperature. Equation 8 gives the $\Delta G°(T)$ curves shown in Figure 5. T_d is the temperature at which the $\Delta G°(T)$ curve crosses the full-drawn straight line ($= -RT \ln(2c)$) because the protein concentrations are kept constant in the consecutive experiments. The extrapolation of the line to the lower temperature side in Figure 4 does not cross the points of cold denaturation, nor does the extrapolation of the $\Delta G°(T)$ curve in Figure 5 predict the experimentally obtained T'_d. Furthermore, ΔC_p for cold denaturation obtainable from the slope of Figure 4 is much smaller than that for the heat denaturation, indicating that the cold denaturation of SSI cannot be explained by the assumption that the secondary structure of SSI in the cold- and heat-denatured states are the same.

Figure 6a shows the plot of T_d and T'_d against pH. T_d was found to increase linearly with increasing pH for heat denaturation, whereas T'_d decreased linearly with increasing pH

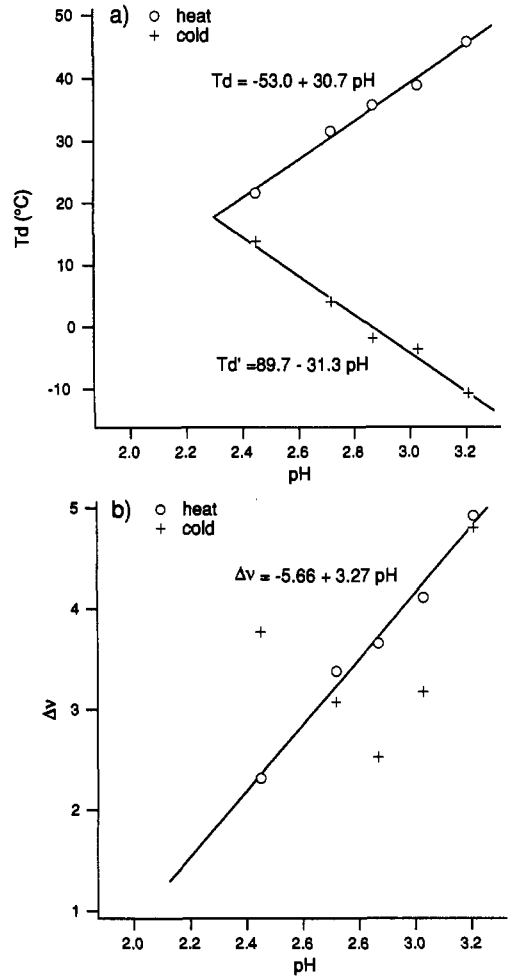

FIGURE 6: (a) Plot of denaturation temperatures of SSI against pH for heat denaturation (O) and cold denaturation (+). (b) Plot of $\Delta\nu$ values obtained from eq 11 against pH for heat denaturation (O) and cold denaturation (+).

for cold denaturation, following the empirical equations obtained by the method of least squares:

$$T_d = -53.0\ (\pm 5.1) + 30.7\ (\pm 1.8)\ \text{pH} \quad \text{heat denaturation} \quad (9)$$

$$T'_d = 89.7\ (\pm 7.0) - 31.3\ (\pm 2.4)\ \text{pH} \quad \text{cold denaturation} \quad (10)$$

If $\Delta\nu$ is the denaturational increase in the numbers of protons bound by the protein per dimer, then

$$\Delta\nu = \frac{\Delta H_{vH}}{2.303RT_d^2}\frac{dT_d}{d\text{pH}} \quad (11)$$

which is derived by differentiating the van't Hoff equation with respect to pH with the assumption that the observed enthalpies exclude the buffer ionization heats, as in the case of the N ⇌ D equilibrium (Privalov, 1979). By eq 11, $\Delta\nu$ is expressed as a function of pH for the heat denaturation as

$$\Delta\nu = -5.66\ (\pm 0.66) + 3.27\ (\pm 0.23)\ \text{pH} \quad (12)$$

but it is difficult to give a similar expression for the cold denaturation (Figure 6b).

From the curve fitting of the CD data at pH 1.84 (Figure 3d), the enthalpy of transition from D′ to D was determined to be 29.8 kcal/mol with a transition temperature of 18.4 °C. The large difference in enthalpy between the D and D′ states shows clearly that they are thermodynamically distinct from each other.

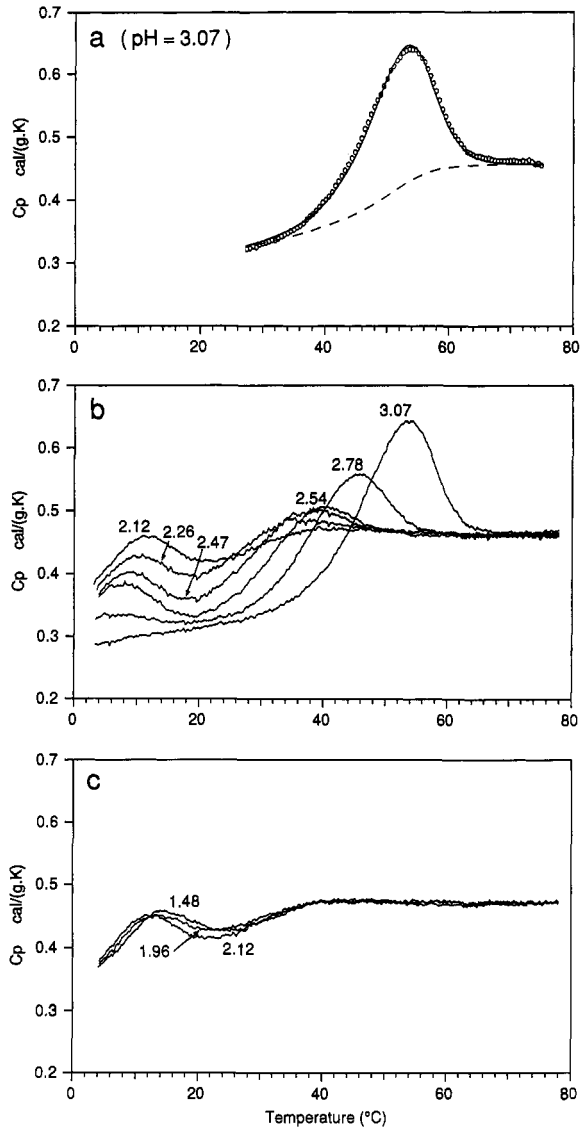

FIGURE 7: (a) Comparison of an experimental (O) and a calculated (—) DSC curve for the heat denaturation of SSI for the model $N_2 \rightleftharpoons 2D$, together with the calculated base line (--). The experimental DSC curve was obtained at a concentration of 3.90 mg/mL in 25 mM glycine buffer, pH 3.07. (b) Experimental DSC curves of SSI at various pH in 25 mM glycine buffers: pH 3.07 (protein concentration, 3.90 mg/mL); pH 2.78 (4.20 mg/mL); pH 2.54 (3.59 mg/mL); pH 2.47 (3.74 mg/mL); pH 2.26 (4.09 mg/mL); pH 2.12 (4.09 mg/mL). (c) Experimental DSC curves at pH 2.12 (protein concentration; 4.09 mg/mL), pH 1.96 (4.03 mg/mL), and pH 1.48 (4.26 mg/mL).

Differential Scanning Calorimetric Measurements. Figure 7a shows a differential scanning calorimetry (DSC) curve of SSI solution at pH 3.07. The experimental data are shown as discrete points by circles, to which the theoretical curve for the equilibrium $N_2 \rightleftharpoons 2D$ was least-squares-fitted by the method of Kitamura and Sturtevant (1989), with the resultant base line shown by the broken line. The accurate fitting indicates that the denaturation of SSI in the acidic pH range can be well expressed as a cooperative reaction involding the equilibrium $N_2 \rightleftharpoons 2D$, as previously pointed out from the concentration dependence of the thermal stability of SSI at pH 7 (Takahashi & Sturtevant, 1981). From this fitting, values of ΔC_p (difference in C_p between the native and the heat-denatured state), ΔH_{cal} (calorimetric enthalpy), and T_d was determined to be 2.02 (±0.15) (kcal/mol·K)), 74.7 (±5.6) (kcal/mol), and 50.2 °C, respectively. These values are slightly different from those obtained from the analysis of CD data. These differences are probably due to the difference in the concentration of SSI in the two types of measurements.

Figure 7b shows DSC curves of SSI at various pH values. At higher temperatures, all the DSC curves converged to a common value, considerably higher than that in the native state, indicating that SSI in the heat-denatured state takes a distinctive state different from the native state irrespective of pH. The peak temperatures and the areas of the DSC curves (corresponding to ΔH_{vH} obtained from CD) for the heat denaturation decreased as the pH decreased, similarly as observed with myoglobin (Privalov et al., 1986) and staphylococcal nuclease (Griko et al., 1988). On the other hand, the peak temperatures for the cold denaturation ($T_{d'}$) increased with decreasing pH much less steeply than those of myoglobin and staphylococcal nuclease, and the area of the excess heat capacity curves for the cold denaturation (corresponding to $\Delta H'_{vH}$) did not decrease as steeply as those of the two proteins. These results suggest that the cold-denatured state of SSI may be different from those of the two proteins which are monomeric and have no disulfide bridges. Also, a much smaller ΔC_p value for the cold denaturation than that for the heat denaturation is inferred from Figure 7b, although a 100% cold-denatured state could not be reached under the present experimental conditions. This result would indicate that SSI retains some tertiary structure in which some hydrophobic amino acid residues are packed in its interior (Privalov & Gill, 1988) as in the native state. As the pH was decreased below 2.0, absorption of heat for the heat denaturation diminished, while that at the position of the cold denaturation did not appear to be diminished at least to pH 1.48 (Figure 7c), with its peak temperature around 12 °C. This indicates that heat absorption of the transition from D′ to D remains even after the native structure is lost, i.e., even after transitions from N to D or D′ disappear. The transition from D′ to D is not much affected by lowering the pH below 2.0 (Figure 7c), probably because the extent of protonation of SSI in the D and the D′ form is the same. Granting that the transition observed below pH 2 is that from D′ to D, the pH dependence of the DSC curves for cold denaturation in Figure 7b can be explained by the assumption that the apparent constancy in the area (corresponding to enthalpy for cold denaturation) with decreasing pH is due to the increased fraction of the transition from D′ to D in addition to that from D′ to N.

The results of the DSC data indicate that the transitions from N to D, N to D′, and D′ to D of SSI are distinctive phase transitions accompanied by the absorption of heat upon increasing temperature. The heat capacity value of SSI in the cold-denatured state is closer to that in the native state, suggesting the presence of a tertiary structure with packed hydrophobic amino acid residues. In contrast, the CD data indicate that the secondary structure is lost in the cold-denatured state to a similar extent as that in the heat-denatured state, although the secondary structures of the two denatured states are not identical. These observations prompted us to investigate the tertiary structure of SSI in the two denatured states and the native state by ^{1}H NMR spectroscopy (Tamura et al., 1991).

ACKNOWLEDGMENTS

We are indebted to Prof. Makino and Mr. Nagahara of Kyoto Institute of Technology, to Prof. Hirose of Institute for Chemical Research of Kyoto University for the use of CD spectropolarimeters, and to Prof. Takahashi and Dr. Fukada of University of Osaka Prefecturte for the use of DASM-4 scanning microcalorimeter. We thank Dr. Kitamura of Kyoto Prefectural University for the use of the program for the curve fitting of calorimetric data and Mr. Noguti for his technical

assistance in analyzing the CD data. We appreciate the reviewers' helpful comments and suggestions.

Registry No. SSI, 120433-50-3.

REFERENCES

Brandts, J. F., & Hunt, L. (1967) *J. Am. Chem. Soc. 89*, 4826.
Griko, Yu. V., Privalov, P. L., Sturtevant, J. M., & Venyaminov, S. Yu. (1988) *Proc. Natl. Acad. Sci. U.S.A. 85*, 3343-3347.
Hiromi, K., Akasaka, K., Mitsui, Y., Tonomura, B., & Murao, S. (1985) *Protein Protease Inhibitor—The Case of Streptomyces Subtilisin Inhibitor* (SSI), Elsevier, Amsterdam.
Johnson, W. C., Jr. (1990) *Proteins: Struct., Funct., Genet. 7*, 205-214.
Kitamura, S., & Sturtevant, J. M. (1989) *Biochemistry 28*, 3788-3792.
Pace, N. C., & Tanford, C. (1968) *Biochemistry 7*, 198-208.
Privalov, P. L. (1979) *Adv. Protein Chem. 33*, 167-241.
Privalov, P. L., Griko, Yu V., Venyaminov, S. Yu., & Kutyshenko, V. P. (1986) *J. Mol. Biol. 190*, 487-498.
Privalov, P. L., & Potekhin, S. A. (1986) *Methods Enzymol. 131*, 4-51.
Privalov, P. L. (1989) *Annu. Rev. Biophys. Biophys. Chem. 18*, 47-69.
Privalov, P. L., & Gill, S. J. (1988) *Adv. Protein Chem. 39*, 191-234.
Sato, S., & Murao, S. (1973) *Agric. Biol. Chem. 37*, 1067-1074.
Tamura, A., Kimura, K., & Akasaka, K. (1991) *Biochemistry* (following paper in this issue).
Takahashi, K., & Sturtevant, J. M. (1981) *Biochemistry 20*, 6185-6190.

Cold Denaturation and Heat Denaturation of *Streptomyces* Subtilisin Inhibitor. 2. ^{1}H NMR Studies†

Atsuo Tamura, Kazuo Kimura, and Kazuyuki Akasaka*
Department of Chemistry, Faculty of Science, Kyoto University, Kyoto 606, Japan
Received May 29, 1991; Revised Manuscript Received August 14, 1991

ABSTRACT: Structural transitions of the protein *Streptomyces* subtilisin inhibitor (SSI) from the native state to the cold-denatured and heat-denatured states were studied by ^{1}H NMR spectroscopy in the temperature range from −10 to 60 °C in the acidic pH range. Assignments of some of the ^{1}H NMR signals of SSI in the cold-denatured and heat-denatured states were performed by a combined use of selective deuteration and site-directed mutagenesis. Throughout the pH range from 2.1 to 3.1, both transitions were cooperative and basically only three distinct spectra corresponding to structures in the cold-denatured, native, and heat-denatured states were detected. In the cold-denatured state, the side-chain signals of Met73, His106, at least one Val, and two Leu were observed at distinctly shifted positions from those for a random-coiled structure, suggesting the formation of a tertiary structure, while those of Met70, His43, and Ala2 were observed at positions for a random-coiled structure. This tertiary structure in the cold-denatured state is entirely different from that in the native state, as some amino acid residues exposed to the solvent in the native state (e.g., Met73, His106) are buried while those sequestered in the native state (e.g., His43) are exposed. In the heat-denatured state, however, most ^{1}H NMR signals were observed at random-coiled positions, indicating that there is much less tertiary structure in the heat-denatured state than in the cold-denatured state. At pH values below 2.09, a structural transition was observed from the cold-denatured state to the heat-denatured state without passing through the native state. A sedimentation equilibrium experiment indicated that the two subunits of SSI were dissociated in both the heat-denatured and cold-denatured states, eliminating the possibility of formation of a tertiary structure in the cold-denatured state by intersubunit interaction, such as by aggregation.

The preceding paper using circular dichroism (Tamura et al., 1991b) indicated that neither the cold-denatured (D′) nor the heat-denatured state (D) of *Streptomyces* subtilisin inhibitor (SSI;[1] see Figure 1 for the tertiary structure) is perfectly random coiled and that the two states differ slightly but distinctly in their secondary structure. Furthermore, DSC experiments suggested that a tertiary structure might be formed from hydrophobic amino acid residues in the D′ form of SSI.

In the present paper, a detailed study of the structural transitions of SSI was undertaken using ^{1}H NMR spectroscopy, which reflects the tertiary structure of a protein more directly than CD and DSC. Our points of interest here are (1) whether SSI takes three distinct states, N, D, and D′, differing in their tertiary structure, (2) whether and how the tertiary structure of SSI in the D′ state is different from that in the D state, and (3) whether the transitions of tertiary structures between the N and D′ forms (cold denaturation),

† This work was supported by a Grant-in-Aid for Developmental Scientific Research from the Ministry of Education, Science, and Culture of Japan.

[1] Abbreviations: SSI, *Streptomyces* subtilisin inhibitor; NMR, nuclear magnetic resonance; CD, circular dichroism; DSC, differential scanning calorimetry.

0006-2960/91/0430-11313$02.50/0